Computers and Electrical Engineering 76 (2019) 198–212

Contents lists available at ScienceDirect

Computers and Electrical Engineering

journal homepage: www.elsevier.com/locate/compeleceng

Analysis of electroencephalographic signals complexity regarding Alzheimer's Disease☆

Katerina D. Tzimourta[a], Theodora Afrantou[b], Panagiotis Ioannidis[b], Maria Karatzikou[b], Alexandros T. Tzallas[c], Nikolaos Giannakeas[c], Loukas G. Astrakas[a], Pantelis Angelidis[d], Evripidis Glavas[c], Nikolaos Grigoriadis[b], Dimitrios G. Tsalikakis[d], Markos G. Tsipouras[d,*]

[a] Department of Medical Physics, Medical School, University of Ioannina, Ioannina GR45110, Greece
[b] 2nd Department of Neurology, AHEPA University Hospital, Aristotle University of Thessaloniki, Thessaloniki GR54636, Greece
[c] Department of Informatics and Telecommunications, School of Informatics and Telecommunications, University of Ioannina, Arta GR47100, Greece
[d] Department of Informatics and Telecommunications Engineering, University of Western Macedonia, Kozani GR50100, Greece

ARTICLE INFO

Article history:
Received 25 November 2018
Revised 28 March 2019
Accepted 28 March 2019
Available online 5 April 2019

Keywords:
Quantitative electroencephalogram
Alzheimer's Disease
Mini-Mental State Examination
MMSE
EEG
AD
Dementia
Complexity

ABSTRACT

Alzheimer's Disease (AD) is the most common type of dementia with world prevalence of more than 46 million people. The Mini-Mental State Examination (MMSE) score is used to categorize the severity and evaluate the disease progress. The electroencephalogram (EEG) is a cost-effective diagnostic tool and lately, new methods have developed for MMSE score correlation with EEG markers. In this paper, EEG recordings acquired from 14 patients with mild and moderate AD and 10 control subjects are analyzed in the five EEG rhythms (δ, θ, α, β, γ). Then, 38 linear and non-linear features are calculated. Multiregression linear analysis showed highly correlation of with MMSE score variation with Permutation Entropy of δ rhythm, Sample Entropy of θ rhythm and Relative θ power. Also, the best statistically significant regression models in terms of R^2 are at O2 (0.542) and F4 (0.513) electrodes and at posterior (0.365) and left-temporal cluster (0.360).

1. Introduction

Alzheimer's Disease (AD) is a progressive chronic brain disease and the most usual type of dementia. AD is characterized by abundant amyloid plaques, neurofibrillary tangles, neuropil threads, and dystrophic neurites as well as neuronal loss or synaptic dysfunction [1]. The main symptoms of AD are memory loss, cognitive abilities damage and behavioral problems in general. In 2015, it was reported [2] that over 46 million patients suffer from dementia worldwide with an estimated increment to 131.5 million patients by 2050. AD restrains the ailing individual and impairs the quality of the patient's life.

The diagnosis of AD is done with several routine medical diagnostics. Mental status is examined with a cognitive questionnaire performed by neurophysiologists and assessed in a 30-point scale named Mini-Mental State Examination (MMSE)

☆ This paper is for CAEE special section SI-ns. Reviews processed and recommended for publication to the Editor-in-Chief by Guest Editor Dr. Victor Albuquerque.

* Corresponding author.
E-mail address: mtsipouras@uowm.gr (M.G. Tsipouras).

https://doi.org/10.1016/j.compeleceng.2019.03.018
0045-7906/

Table 1
EEG findings for Alzheimer's Disease, based on the features that are most recommended in the literature. Alterations in EEG features of AD patients compared to healthy subjects are depicted with increase/decrease arrows.

Alterations in EEG recordings of AD patients	EEG activity	Brain region
↑ power of δ and θ bands [16–18]	slowing	temporal, parietal, and occipital regions.
↑ delta modulations of δ band across [6]	slowing	temporal, parietal, and occipital regions.
↓ power of higher bands [16]	slowing	entire brain
↓ alpha modulation [19]	slowing	parietal region
↓ auto-mutual information [9]	complexity	T5, T6, O1, O2, P3, P4
↓ Approximate Entropy [9]	complexity	O1, O2, P3, P4
↓ Permutation entropy [7,8]	complexity	temporal, parietal, and occipital regions.
↓ Sample Entropy [11]	complexity	O1, O2, P3, P4
↓ Tsallis Entropy [20]	complexity	C7, T7
↓ Multiscale Entropy [4,13]	complexity	entire brain
↓ correlation dimension [10]	complexity	F3, F4, F8, Fp1, Fp2, C3, C4, T3, T4, T6, P3, P4, O2
↓ 1st positive Lyapunov exponent [10]	complexity	F3, F4, F8, Fp1, Fp2, C3, C4, T3, T4, T6, P3, P4, O2
↑ Ω (global complexity) [21]	complexity	entire brain
↓ Lempel–Ziv Complexity [11]	complexity	entire brain
↑ stochastic event synchrony measures [14]	synchrony	entire brain
↓ Granger causality [14]	synchrony	entire brain
↓ state space-based synchronization measures [14]	synchrony	entire brain
↓ magnitude and phase coherence [14]	synchrony	entire brain

with lower MMSE indicating more severe cognitive decline. Brain imaging with magnetic resonance imaging (MRI) or computed tomography (CT) and Electroencephalographic (EEG) recording are also performed along with general neurological and physical examination [3].

Over the past decades, the EEG as a cost-effective diagnostic method, has become of great scientific interest and various researchers have tried to extract valuable information about dementia. Researchers have focused on analyzing the EEG recordings from AD patients in order to find alterations related to the complexity, the synchrony and the regularity of EEG activity. For this purpose, researchers in several studies have acquired the EEG recordings from AD patients in a clinical environment, while the patients were resting in an upright position [4] or during a cognitive task [5]. Then, the EEG recordings were processed and certain features were extracted, in order to discriminate the AD patients from healthy controls [6–8] or compare the AD characteristics with the ones extracting from age-matched healthy subjects and shed light on the mechanisms and the progression of the disease.

In particular, the EEG complexity in AD patients has concerned the majority of researchers. In previous studies, the auto-mutual information, [9] the correlation dimension [10], the largest Lyapunov exponent [10], the Approximate Entropy [9]), the Permutation entropy [8], the Sample Entropy [11,12], the Tsallis Entropy [13], the Lempel–Ziv complexity [11] have been examined and have revealed perturbations of EEG complexity. Generally, results reported loss of physiological EEG complexity in moderate AD patients in comparison with EEG signals from healthy age-matched subjects. Furthermore, few studies [5,14,15] have tried to detect fluctuations in EEG synchrony from patients' recordings related to AD. In the literature, several synchrony measures have been evaluated including correlation coefficient [14], cross-entropy [14], wavelet entropy [14], state space and divergence measures [14], Multivariate Autoregressive Model (MVAR) coherence [14], coherence [5,15], Granger causality [14], partial coherence [5,14] direct Directed Transfer Function (DFT) [14], phase measures [5,14], canonical correlation, [5,15], conditional Granger causality [5,15], dynamic canonical correlation [5]) and cross-mutual information [5]. In these studies, the authors did not extract results solely for each channel, but they formed pairs [15] or clusters [13,14] of EEG channels, to comprehensively analyze the synchrony and obtain results, which are more representative to clinical practice. Results indicated that the left hemisphere is mostly affected [13,16] and there is a decrease in EEG synchrony in AD patients, mostly in patients with moderate AD [5] compared to healthy individuals.

With regard to the regularity of EEG activity that have been reported, studies have shown that there is a slowing of brain activity, meaning that the power of higher EEG bands is decreased and the power of lower EEG bands is increased. Many studies have reported a decrease of the relative α band power and an increase of δ band power [17] and especially in severe AD patients [18]. Also, an increase in θ band power in mild AD [18] and decrease of δ modulations of the δ frequency band across temporal, parietal, and occipital regions [19] has been observed. Furthermore, decrease of higher bands power and amplitude modulation in parietal regions [19] and especially of α band in moderate AD patients [18] have been reported.

The effects of the AD are mainly shown in occitoparietal and temporal regions and in α and θ bands ([6, 7]). This interesting fact indicates that the slowing of the EEG in these areas correspond to the degeneration of these regions in AD patients [7]. Table 1 presents a concise overview of the EEG alterations based on the features that are mostly proposed in the literature, along with the aspects of the EEG that each feature represents.

1.1. Related work

Recently, a new field of research has emerged and researchers have addressed the problem of correlating the cognitive decline through the MMSE score with the EEG features from the AD patients. In [4] the authors investigated the appropriate

parameters m and r of multiscale entropy and examined the correlation of multiscale entropy with cognitive dysfunction. For this purpose, EEG epochs of 30 s acquired from 108 AD patients were analyzed, forming a 1-hour-long database for analysis. Three groups of pathological EEG data were formed according to the severity of the disease (mild, moderate and severe). The authors examined the best range of scale factor in multiscale entropy and performed a partial correlation analysis. The post-hoc statistical analysis showed that patients with moderate to severe AD showed the lowest multiscale entropy for scale factors 1 to 6 in most electrodes and the highest multiscale entropy for scale factors 16 and 20 in posterior electrodes. Also, the multiscale entropy of EEG in temporal and occipitoparietal electrodes was correlated with MMSE score.

The amplitude modulation is another feature examined in a recent study [19]. EEG recordings from 76 participants (27 healthy controls, 27 patients with mild AD and 22 with moderate AD) were analyzed with Hilbert Huang Transform and the cross-frequency amplitude modulation interaction was computed. The results concerning the progression of the disease severity indicated a decrease in beta band amplitude modulation in temporal, parietal, and occipital regions and increased theta band amplitude modulations.

Researchers have recently shown interest on associating the disease severity and particularly the MMSE score with EEG findings ([5, 13, 15]). The multi-centric Prospective Dementia Database Austria (PRODEM) has been employed in all these studies. The EEG was recorded both in resting state with eyes closed and during an encoding task. For this study([15, 22]), 118 patients with possible or probable AD were recruited. The EEG recording of each patient lasted about 158 s and it segmented in epochs of 4-s with 2-s overlap. The authors estimated several features to examine the reduced complexity, the altered synchrony and the slowing of EEG patterns in AD and associated the MMSE score with relative θ power, coherence, canonical correlation, auto-mutual information, Shannon and Tsallis entropy. The coherence and canonical correlation associated with MMSE score and also, the relative θ power and the auto-mutual information were increased in EEG recordings from AD patients. In a similar study [5] of 79 subjects with probable AD, the EEG was acquired in both resting state and during a cognitive task. The quadratic least-squares regression was employed for the correlation of the EEG synchrony changes with severity of AD as measured by MMSE score. The authors examined the EEG synchrony in electrode clusters. Results showed that the synchrony between Anterior-Temporal/Left, Posterior-Temporal/Left and Posterior-Temporal/Right EEG channel groups were most significantly related with AD severity. Furthermore, the EEG synchrony was increased for MMSE score above 20 and decreased for MMSE below 20. Similarly, [13] the auto-mutual information (AMI) and several entropy features (Shannon, Tsallis, Multiscale, Spectral) were examined and results showed a decline in AMI, Spectral entropy and Multiscale Entropy as the disease was progressing.

In this study, we extract several features from EEG recordings from patients with mild AD, moderate AD and subjects without dementia and examine their correlation with MMSE score. The features are both statistical and spectral and most of the them have been proposed independently for MMSE correlation. The objective of this study is to find specific EEG markers from a group of linear and nonlinear features associated to MMSE score.

The paper is organized as follows: In Section 2 the methodology and the extracted EEG features are addressed. Section 3 presents the obtained results and the MMSE score predictors and Section 4 discusses the obtained results compared to literature findings. Finally, the conclusion of the study is presented in Section 5.

2. Materials and method

EEG recordings from 24 subjects,14 patients with AD (5 with moderate AD and 9 with mild AD) and 10 healthy subjects are analyzed. Then, 38 spectral and statistical features are calculated and a Multiple Regression analysis is performed in order to examine the model of features that best correlates with the MMSE.

2.1. Database description

In this study, 24 subjects participated from the 2nd Department of Neurology of AHEPA General University Hospital of Thessaloniki. Cognitive and neuropsychological state was evaluated by the international Mini-Mental State Examination (MMSE) and Clinical Dementia Score (CDR). MMSE score ranges from 0 to 30, with lower MMSE indicating more severe cognitive decline, whereas CDR is a 5-point scale (0, 0.5, 1, 2, 3) with higher score representing a severe AD. The 24 participants formed three groups depending their MMSE score: Controls, Mild AD and Moderate AD. Fourteen patients (8 females and 6 males) were diagnosed with AD, from which 6 patients with moderate AD (MMSE score 14 - 16) and 8 with mild AD (MMSE score 18 – 23), whereas 10 subjects formed the control group. The duration of the disease was measured in months and the median value was 25 with IQR range (Q1-Q3) being 28.5 - 24 months. Concerning the AD groups, no dementia-related comorbidities have reported. The average MMSE and CDR for the AD groups was 20 (16–21.5) and 1 (0.625–2) respectively and for controls 30 and 0, apparently. Also, participants among the groups had approximately the same age: 62.5 (61.25–68.25) for moderate AD, 73.5 (77.25–68.5) for mild AD and 67 (72–62.25) for controls. The education level was recorded for each participant on a scale ranging from 6 to 16 years corresponding to primary (6 years), secondary (12 years) and higher education (16 years). Statistical significance analysis has been performed between the three groups with Welch ANOVA concerning age ($p\text{-}value{=}0.124$, $F(2,21){=}2.473$) and with non-parametric Kruskal-Wallis test for MMSE score ($\chi^2 = 21.913$, $p - value < 0.001$, with mean rank MMSE of 19.5 for controls, 10.5 for mild AD and 3.5 for moderate AD). Analysis was established to ensure that there are not statistically significant differences between subject groups (Controls, mild AD patients

Table 2
Description of patients' demographic characteristics along with the neuropsychological factors.

Demographic characteristics				Neuropsychological factors			
Patient	Gender	Age	Level of Education	MMSE	CDR	Duration of illness (months)	Disease stage (severity)
1	female	57	secondary	16	2	48	Moderate
2	female	77	secondary	23	0.5	12	Mild
3	female	79	primary	20	1	24	Mild
4	female	78	primary	22	0.5	18	Mild
5	male	70	higher	22	0.5	24	Mild
6	female	77	primary	14	2	36	Moderate
7	male	63	primary	18	1	24	Moderate
8	male	69	primary	20	1	30	Mild
9	female	67	secondary	20	1	24	Mild
10	male	71	primary	22	0.5	24	Mild
11	male	62	secondary	16	2	24	Moderate
12	female	64	higher	20	1	12	Mild
13	male	70	primary	14	2	24	Moderate
14	female	61	secondary	14	2	36	Moderate
Total	8 females 6 males	–	7 primary 5 secondary 2 higher	–	–	–	6 Moderate 8 Mild
Median (IQR)	–	69.5 (63.25–75.5)	–	20 (16–21.5)	1 (0.625–2)	25.00 (28.5–24.0)	–

and moderate AD patients) regarding age and that there is a significant association between the 3 groups and the MMSE score. Table 2 presents a description of patients' characteristics.

2.2. Data acquisition

The EEG recordings were performed in the EEG examination room of the 2nd Department of Neurology of AHEPA General University Hospital of Thessaloniki by an experienced team of neurologists. Each participant received a routine EEG recording in the Nihon Kohden EEG 2100 device. The electrode placement was in accordance to 10–20 International Reference System and 19 electrodes were used (Fp1, Fp2, F7, F3, Fz, F4, F8, T3, C3, Cz, C4, T4, T5, P3, Pz, P4, T6, O1 and O2) and 2 reference electrodes placed in the participant's earlobes (A1 and A2) for skin-electrode impedance check, according to the manual of the device. Vertical electro-oculogram (EOG) was recorded by electrodes placed above and below the right eye and horizontal electro-oculogram (EOG) was recorded by electrodes placed at the outer corner of the left eye. The recording montages were anterior-posterior bipolar and referential montage using Cz as the common reference and the anterior-posterior montage was used for the analysis. The recordings were received under the range of the following parameters of the amplifier: Sensitivity: 10μV/mm, time constant: 0.3 s, and high frequency filter at 70 Hz. Participants were in an upright seated position, in a resting state with their eyes closed. Each recording was sampled at 500 Hz and lasted approximately 13 min (ranging from 11 to 17 min) for AD patients and approximately 21 min (ranging from 20 to 23 min) for control group. In total, 179 min of EEG recordings from AD patients and 188 min with normal EEG data were collected, forming a database of approximately 6 h.

2.3. EEG signals processing

The EEG recordings are exported in ".eeg" format and are processed using Matlab platform and the EEGLAB toolbox. The log file as exported by the Nihon Kohden EEG 2100 device, provided information about any possible artifacts during each EEG recording (muscle activity, blinking, swallowing), which are marked and removed. In the analysis, EEG information is extracted concerning anterior-posterior longitudinal bipolar montage (also known as "double banana"), which is the most commonly used montage in clinical practice. Longitudinal bipolar montage is an appropriate montage to see the symmetry of EEG dynamics between regions of the two hemispheres and the α rhythm in the occipital region and provides less external noise compared with referential montage. Afterwards, a Butterworth notch filter is applied to remove the 50 Hz power line noise oscillations from the EEG recordings and a high-pass FIR (Equiripple) digital filter with a cut-off frequency at 0.5 Hz to remove low frequency oscillations. Then, each filtered EEG recording is segmented in non-overlapping epochs of 10 s in line with study [8] and statistical features are extracted from the 10-s EEG segments. In order to extract spectral features in each frequency sub-band of interest, five equiripple FIR filters are designed using the FIRPM function and applied to each 10-s EEG segment. Therefore, five band-pass filters (0.5–4 Hz, 4–8 Hz, 8–13 Hz and 13–30HZ, 30–60 Hz) are designed.

2.4. Feature extraction

In the literature, a variety of features has been suggested to elucidate the EEG waveforms related to Alzheimer's Disease. In the present study, six statistical features are extracted from the 10-s segments, five spectral features are calculated in each sub-band of interest corresponding to the five EEG rhythms (δ, θ, α, β and γ) and 2 spectral features calculated for the entire frequency spectrum.

Six statistical features are calculated for each data segment x_j of length N, namely:

$$\text{Mean}, \bar{x} = \frac{1}{N}\sum_{j=1}^{N} x_j, \;\; \text{j} = 1, 2, \ldots \text{N} \tag{1}$$

which is the sum of the series of variables divided by the number of variables. In statistics, the mean estimates the central tendency of a probability distribution of a variable, meaning the tendency of the data to cluster around some central data. The mean is a basic measure and many statistical metrics rely their calculation upon it.

$$\text{Variance}, \sigma^2 = \frac{1}{N\ -\ 1}\sum_{j=1}^{N}\left(x_j - \bar{x}\right)^2 \tag{2}$$

which is the mean square deviation of a data segment x_j from its mean value. In statistics, the variance is the second moment of distribution and it actually represents the width of data around its central value, the mean.

$$\text{Standard deviation (STD)}, \sigma = \sqrt{\frac{1}{N\ -\ 1}\sum_{j=1}^{N}\left(x_j - \bar{x}\right)^2} \tag{3}$$

which is the square root of variance. Same as variance, standard deviation is a measure of dispersion of the data around its mean. Low values of σ indicate that the distribution is extending with less width around the mean and data points close to the central value; however, high values of σ indicate wider dispersion.

$$\text{Skewness}, \gamma_1 = \frac{1}{N}\sum_{j=1}^{N}\left[\frac{x_j - \bar{x}}{\sigma}\right]^3 \tag{4}$$

which is the mean cube deviation of a data segment x_j from its mean value divided by its standard deviation. Skewness is the third moment of distribution of a data segment and estimates the degree of asymmetry around the mean. Positive values of skewness indicate that graphically the long tail of distribution is extending towards positive values of x regarding the mean and negative values of skewness indicate asymmetry of distribution towards negative values of x.

$$\text{Kurtosis}, \gamma_2 = \frac{1}{N}\sum_{j=1}^{N}\left[\frac{x_j - \bar{x}}{\sigma}\right]^4 \tag{5}$$

which is the mean deviation of a data segment x_j from its mean value divided by its standard deviation and raised in the power of 4. Kurtosis originated with Karl Pearson and is the forth moment of distribution. In statistics, kurtosis estimates how peak or flat a distribution of a signal is regarding a normal distribution. Positive values of kurtosis represent graphically a sharper distribution with regard to a normal distribution (leptokurtic) and negative values of kurtosis represent a flatter distribution (platykurtic).

$$\text{Interquartile Range (IQR)}, IQR = Q_3 - Q_1 \tag{6}$$

which is the difference between Q_1 and Q_3, also known as 25th percentile (lower) and 75th percentile (upper) respectively. The quartiles are calculated based on the median of the data. Thus, in a probability distribution, Q_1 is calculated from the median of the lower half of the data and Q_3 from the median of the upper half of the data.

Furthermore, several spectral features are calculated for each segment x_j. Entropy measures generally characterize the level of complexity and predictability of a signal. For each data segment x_j of each channel, FIR filters are applied decomposing each segment into five sub-bands i of interest corresponding to the five EEG rhythms (δ, θ, α, β, γ). Then, spectral features are extracted in each band and the normalized value (ranging from 0 to 1) of each feature is calculated, aiming to optimize the comparison between different AD states. The normalized value of each feature is calculated by dividing the feature value of each band with the total feature value, meaning the sum of features calculated for all the frequency bands.

$$\text{Energy}: Energy_i = \sum_{j=1}^{N} x_j^2, i = \delta, \theta, \alpha, \beta, \gamma \tag{7}$$

which is the square value of a data segment x_j calculated for each band i.

$$\text{Relative band power (RBP)}, RBP_i = \frac{Energy_i}{\sum Energy_i}, i = \delta, \theta, \alpha, \beta, \gamma \tag{8}$$

which is based on the periodogram of the segment and shows in percentage the normalized distribution of the power in each band concerning the total segment power.

$$\text{Shannon entropy}, ShanEn = -\sum_{j=1}^{M} p_j \log\left(p_j\right), \tag{9}$$

wherein p_j is the probability distribution of each data segment x_j and is calculated estimating the histogram for each segment. ShanEn is a measure of complexity and is calculated for the entire frequency spectrum.

$$\text{Approximate entropy (ApEn)},\ ApEn(m,r,N)_i = -\left[\varphi^{m+1}(\mathrm{r}) - \varphi^{m}(\mathrm{r})\right], i = \delta, \theta, \alpha, \beta, \gamma \tag{9a}$$

where $\varphi^m(\mathrm{r}) = \sum_{k=1}^{N-m+1} \frac{ln\ c_r^m(k)}{N-m+1}$ and c_r^m a correlation integer $c_r^m(k) = \frac{count\ \{\ d(k,l)\ \le\ r\}}{N-m+1}$ estimated by the distance $d(k, j)$ between the vectors $u(k) = [x(k), x(k+1), \ldots, x(k+m-1)]$ and $u(l)$.

According to Pincus [23], m (pattern length) is usually 1 or 2 and r (similarity factor) takes values 0.1, 0.15, 0.25 and 0.5. Generally, it has not been proposed a specific value for each variable, optimizing ApEn. In our experiments, $m = 1$ and $r = 0.2$ times the standard deviation of the time-series in accordance with the study [9]. High values of ApEn mean low predictability of a segment to be followed by a similar data segment; thus, high values of ApEn characterize more complex and irregular waveforms. However, low values of ApEn are an indicator of a simpler and more predictable signal, since it is assumed that it is more probable for a data segment to be followed by similar data segments.

$$\text{Permutation entropy},\ PermEn_i = -\int p(\pi)\log\ p(\pi), i - \delta, \theta, \alpha, \beta, \gamma \tag{10}$$

wherein π are all the permutations of order n, which is the number of embedding dimensions and $p(\pi)$ is the probability of ordinal patterns π, meaning the relative frequency of ordinal patterns π. PermEn is similar to ShanEn for ordinal patterns and is a complexity measure proposed by Bandt & Pompe [24] for arbitrary, noisy and large signals. According to their study, n takes values $n = 3, \ldots, 7$. In our experiments, n is assigned to 3.

$$\text{Tsallis entropy (TsalEn)},\ TsalEn_i = \frac{1}{q-1}\left(1 - \sum\nolimits_u^W p_u^q\right), i = \delta, \theta, \alpha, \beta, \gamma \tag{11}$$

where q is any real number measuring the degree of nonextensivity with $q < 1$ for superextensive and $q > 1$ for subextensive statistics, whereas $q = 1$ gives the ShanEn. TsalEn is a non-extensive entropy, meaning that the entropy of the system (i.e. a time-series) is not correlated with the entropy of each subsystem; hence, is not the sum of entropy measures of each subsystem [25]. In our experiments, $q = 2$ since EEG is considered a subextensive system (i.e., $q > 1$).

Which is a variation of SamplEn for the scaled signal. MSE was proposed by Costa [26] mainly to overcome difficulties and misleading results for physiological signals. MSE introduces a range for multiple time scales τ, which is used to construct a coarse-grained version of the original time series. The original signal is divided in windows of length τ and the data of each window is averaged. Each element of the coarse-grained signal is calculated based on the formula:

$$\text{Multiscale entropy (MSE)}\ y_j^{(\tau)} = \frac{1}{\tau}\sum\nolimits_{k=(j-1)\tau+1}^{j\tau} x_k, \quad 1 \le j \le N/\tau \tag{12}$$

For $\tau = 1$ the equation gives the original signal. Generally, Costa et al. proposed a range of values $m \in [1,2]$, $r \in [0.10, 0.15, 0.20, 0.25, 0.50]$ (described above for Approximate Entropy) and $\tau \in [2 \ldots 20]$ as well as many other researchers [4]. In our experiments, $m = 2$, $r = 0.15$ and $\tau = 5$ after examination of several combinations for m, r and τ and are consistent with previous studies [4,26]. However, the objective of the proposed study is not to find the best combination optimizing multiscale entropy and hence, an exhaustive examination of various combinations of m, r, t, is not presented. MSE is calculated for the entire frequency spectrum.

$$\text{Sample entropy (SamplEn)},\ SamplEn\ (m,r,N)_{\ i} = -ln\frac{\varphi^m(\mathrm{r})}{\varphi^{m+1}(\mathrm{r})}, i = \delta,\ \theta,\ \alpha,\ \beta,\ \gamma \tag{13}$$

where $\varphi^m(\mathrm{r}) = \sum_{i=1}^{N-m+1} \frac{c_r^m(i)}{N-m+1}$ and $c_r^m(i) = \frac{count\ \{\ d(i,j)\ \le\ r\}_{i \ne j}}{N-m+1}$ estimated by the distance $d(k, l)$ between vectors $u(k) = [x(k), x(k+1), \ldots, x(k+m-1)]$ and $u(l)$. SamplEn is similar to ApEn but it does not include the estimation of self-similar patterns. The algorithm of Sample entropy does not include the calculation $d(k, l)$ for $k = l$, while calculating the distance $d(k, l)$ between the vectors $u(k)$ and $u(l)$ [27]. Therefore, ApEn presents a more regular system than the system actually is. In our experiments, $m = 2$ and $r = 0.15$ as proposed in [4]

2.5. Statistical analysis

In order to examine the association between each of the 38 extracted features with the severity of the Alzheimer's Disease and particularly the MMSE score, Multiregression Linear Analysis is conducted using the IBM SPSS Statistics platform. Regression models are created separately for each channel and for clusters of channels, which are created according to the electrode placement and the corresponding brain regions. The five electrode clusters namely Anterior (Fp1, F3, Fz, Fp2, F4), Posterior (P3, O1, Pz, P4, O2), Central (C3, Cz, C4), Temporal/left (T3, T5, F7) and Temporal/right (T4, T6, F8) are defined in previous studies ([14, 5]). In these models, the MMSE score served as the dependent variable and each EEG feature as the independent/predictor. All the assumptions of Linear Regression are examined (data normality, linearity, independence, homoscedasticity, multicollinearity and residuals normality) and the stepwise method is chosen, wherein the predictors of the model are chosen based on the largest Pearson correlation. Finally, ANOVA analysis is also performed to evaluate the significance of the obtained models and results are presented below. Normality and homogeneity of variances were examined with Shapiro-Wilk test and Levene's test respectively. In Fig. 1 the electrode clusters are shaded in different colors.

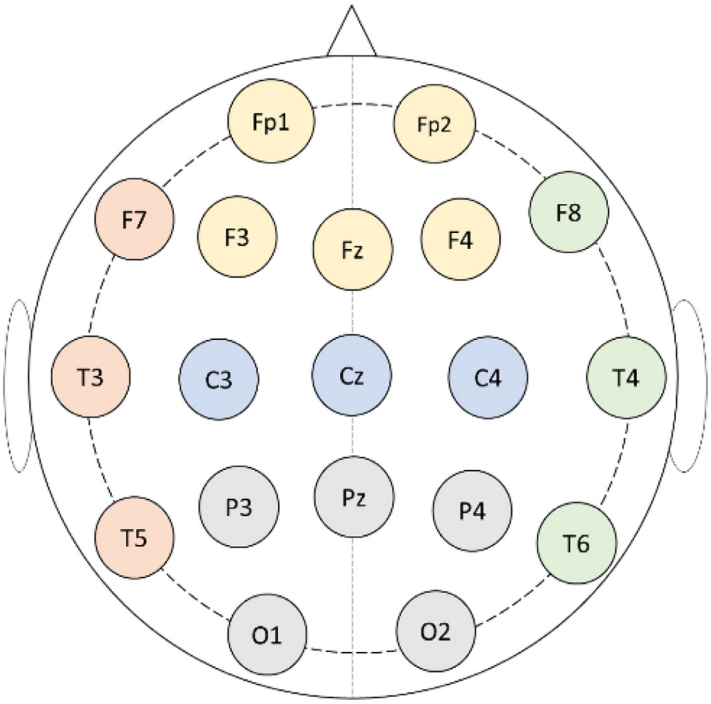

Fig. 1. Electrode clusters according to the electrode sites. Anterior cluster is shaded with yellow, central cluster is shaded with light blue, posterior cluster is shaded with grey, temporal right and left cluster are shaded with orange and light green, respectively.

Table 3
Regression results in terms of R^2 for each electrode cluster.

Electrode cluster	highest R^2	*P-value*
Anterior (Fp1, F3, Fz, Fp2, F4)	0.293	0.000
Central (C3, Cz, C4)	0.335	0.009
Temporal/left (T3, T5, F7)	0.360	0.012
Temporal/right (T4, T6, F8)	0.355	0.000
Posterior (P3, O1, Pz, P4, O2)	0.365	0.000

3. Results

The evaluation of regression models is conducted with the square value of Multiple Correlation Coefficient (R^2), which shows the proportion of variation of the dependent variable (MMSE) explained by the predictor [17]. P-value is also reported to confirm that the null hypothesis is rejected and thus, there is a significant linear association between the dependent and the independent variable ($p\text{-}value<0.05$). The best statistically significant R^2, while avoiding feature multicollinearity for each cluster and for each channel, is presented at Tables 3 and 4, respectively. Each R^2 is chosen only if it is statistically significant ($p\text{-}value<0.05$) and after examining the Variance Inflation Factor (VIF) values for each model. VIF is a statistic for multicollinearity, meaning the ability of an independent variable to be able to predict another independent variable. Multicollinearity occurs when variables are highly correlated with each other and produces misleading results. In the presented results the VIF value is below the accepted value of 10.0 in all models. Also, the significant regression models in terms of standardized Beta weights for each electrode site and electrode cluster are presented in Table 5.

The best R^2 (0.365) of significant regression models is obtained for the posterior cluster, which contains the electrodes P3, O1, Pz, P4 and O2, whereas the worst R^2 (0.293) is shown for the anterior cluster and the electrodes Fp1, F3, Fz, Fp2, F4. The left temporal cluster (T3, T5, F7) also showed good computed R^2 (0.360) followed by the right temporal cluster (T4, T6, F8), wherein the R^2 value did not differ much (0.355), and of central cluster with C3, Cz and C4 (0.335).

Multiregression Linear Analysis is also conducted for each electrode individually. The best correlation in terms of R^2 is obtained for electrode O2 (0.542) followed by electrode F4 (0.513), electrode T5 (0.488), electrode O1 (0.478), electrode T6 (0.468), electrode F8 (0.448), electrode P3 (0.441), electrode P4 (0.427), electrode C4 (0.420), electrode Cz (0.420), electrode Pz (0.416), electrode T4 (0.416), electrode F3 (0.412), electrode T3 (0.412), electrode F7 (0.398), electrode C3 (0.397), electrode Fp1 (0.372) and electrode Fz (0.339). The worst value of R^2 and hence lower association with MMSE score showed

Table 4
Regression results in terms of R^2 for each electrode.

Electrode	highest R^2	*P-value*
Fp1	0.372	0.002
F3	0.412	0.017
Fz	0.339	0.004
Fp2	0.202	0.032
F4	0.513	0.000
P3	0.441	0.000
O1	0.478	0.007
Pz	0.416	0.014
P4	0.427	0.002
O2	0.542	0.001
C3	0.397	0.000
Cz	0.420	0.000
C4	0.420	0.001
T3	0.412	0.000
T5	0.488	0.000
F7	0.398	0.000
T4	0.416	0.044
T6	0.468	0.018
F8	0.448	0.004

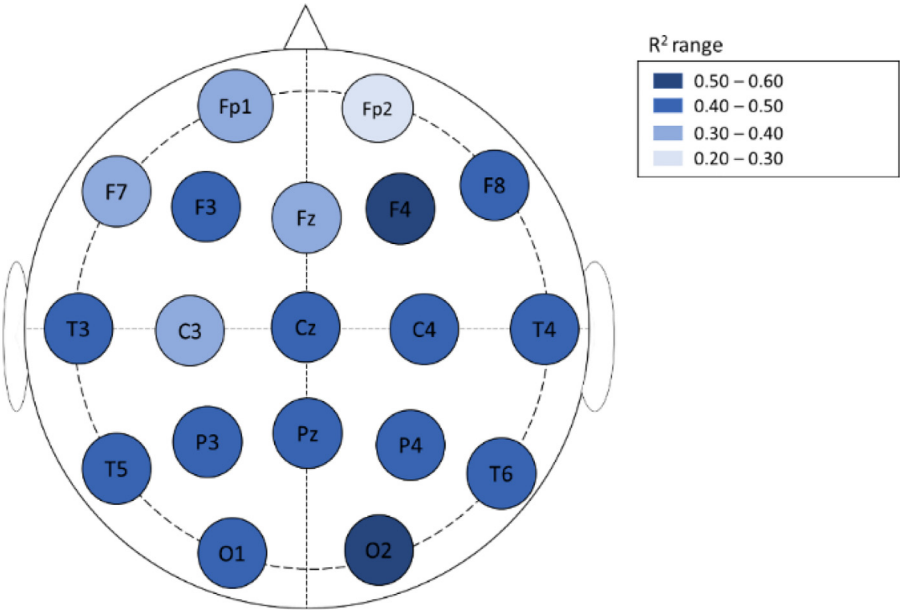

Fig. 2. Depiction of the MMSE correlation with each EEG electrode site according to the obtained results of R^2. The correlation of the predictors of the corresponding channel with MMSE score is illustrated with a colorbar. Lighter shades of blue in electrodes correspond to lower values of R^2, whereas darker shades of blue corresponds to a higher value of R^2 and thus, higher correlation with MMSE.

the electrode Fp2 (0.202). Fig. 2 shows the correlation of each channel in the prediction of MMSE score according to the computed R^2 for each electrode site and Fig. 3 represents the distribution of the obtained R^2 in each EEG channel.

According to Pearson correlation and the obtained regression models, the EEG markers that predicts the variation of MMSE score for all electrodes are presented in Fig. 4. $PermEn_\delta$ is extensively shown in the significant regression model of 16 electrodes. RBP_θ, $SamplEn_\delta$, and Mean are frequently shown in 14 electrodes and $SamplEn_\beta$ is shown in 13 electrodes. In 12 electrodes $PermEn_\beta$ and RBP_γ, is shown and in 10 electrodes the $PermEn_\theta$ and MSE. The rest EEG features are shown in the regression models of less than 10 electrodes.

Furthermore, the correlation of EEG predictors with MMSE in each electrode site, concerning each EEG rhythm is depicted in Fig. 6.

4. Discussion

In this study, a correlation of the variation of MMSE score with EEG features related to the EEG signal complexity is presented. Several statistical and spectral features are extracted from EEG recordings of 10 control subjects, 8 patients with

Table 5
Regression model in terms of standardized Beta weights for each electrode and electrode cluster. Significant results are presented in bold (Beta > 0.3).

Standardized Beta weights																								
Predictor	anterior	posterior	central	temporal	temporal	Fp1	F3	Fz	Fp2	F4	P3	O1	Pz	P4	O2	C3	Cz	C4	T4	T6	F8	T3	T5	F7
$PermEn_{\delta}$	**0.336*****	–	0.132***	0.148***	0.263***	0.233***	0.294***	0.125***	**0.404*******	**0.368*****	0.107***	0.054*	–	0.258***	- 0.103***	0.286***	–	0.280***	0.223***	**0.447*****	0.185***	–	0.290***	0.120***
$SamplEn_{\delta}$	0.087***	0.106***	**0.377*****	0.183***	0.231***	–	–	0.257***	0.180***	0.230***	0.287***	**0.465*****	–	**0.453*****	**0.336*****	**0.315*****	**0.504*****	**0.340*****	**0.654*****	0.155***	**0.559*****	–	0.170***	–
Mean	–	−0.093***	−0.041***	−0.075***	−0.149***	−0.125***	−0.086***	–	–	−0.189***	−0.224***	−0.147***	−0.175***	−0.099***	−0.092***	−0.069***	–	–	−0.114***	−0.135***	−0.157***	–	−0.120***	−0.090***
RBP_{θ}	−0.174***	−0.120***	**−0.362*****	−0.186***	−0.249***	−0.083**	−0.138***	–	−0.200***	–	−0.158***	–	−0.158***	**−0.307*****	−0.146***	**−0.410*****	−0.229***	**−0.402*****	−0.271***	−0.236***	−0.165***	−0.179***	–	–
$SamplEn_{\beta}$	–	–	0.190***	0.151***	–	–	0.181***	0.310***	–	0.194***	0.082**	–	–	**0.348*****	0.119***	0.170***	–	0.141***	0.085*	0.181***	0.148***	–	0.130***	0.298***
$PermEn_{\beta}$	−0.248***	−0.285***	−0.12***	**−0.382*****	−0.206***	**−0.341*****	**−0.358*****	−0.16***	–	−0.265***	−0.209***	**−0.398*****	−0.266***	–	–	–	–	–	−0.231***	–	**−0.477*****	**−0.378*****	−0.170***	**−0.336*****
RBP_{γ}	–	0.244***	0.035*	0.054**	–	0.159***	–	0.169***	–	0.181***	–	**0.437*****	0.195***	0.212***	0.517***	–	–	0.083**	–	0.240***	–	0.140***	**0.360*****	0.210***
$PermEn_{\theta}$	–	0.218***	0.144***	0.075***	–	−0.192***	−0.087**	–	–	–	0.217***	0.284***	–	**0.483*****		0.184***	–	0.153***	0.121***	0.110**	–	–		0.267***
MSE	0.151***	0.087***	0.123***	0.076***	0.142***	–	–	0.086***	–	0.079**	0.095***	0.270***	0.132***		0.254***	0.053***	–	0.099***	–	0.180***	–	–	0.250***	–
$SamplEn_{\alpha}$	–	0.251***	–	0.222***	0.253***	0.152***	–	–	–	0.095**	**0.310*****	0.232***	0.150***	0.148***	–	–	–	–	**0.662*****	–	**0.458*****	**0.351*****	–	–
$Energy_{\gamma}$	–	0.113***	0.099***	–	–	0.207***	0.153***	–	–	0.189***	0.168***	0.174***	–	0.100***	0.469***	–	–	–	0.060*	–	–	–	−0.210***	–
ShanEn	–	–	0.132***	–	–	–	–	–	–	–	0.054**	0.067**	0.075**	–		0.071***	0.147***	0.091***	0.059**	0.054*	–	–	–	–
$SamplEn_{\delta}$	–	–	0.137***	−0.140***	–	−0.272***	–	–	–	−0.25***	–	**0.486*****	0.092***	–	0.429***	–	–	–	–	–	–	**−0.362*****	–	**−0.318*****
Kurtosis	–	–	–	−0.101***	−0.064***	–	–	–	–	−0.051**	–	−0.067***	−0.064***	–	−0.084***	–	–	–	−0.041*	−0.086***	−0.143***	–	−0.070***	–
$ApEn_{\gamma}$	−0.193***	−0.227***	–	–	−0.195***	−0.081**	–	–	–	–	–	–	−0.189***	–	**−0.405*****	−0.267***	–	−0.252***	−0.187***	−0.145***	–	–	–	–
$PermEn_{\alpha}$	–	0.245***	−0.189***	0.084***	–	–	–	−0.214***	–	–	–	0.571***	–	0.080*	0.296***	–	−0.233***	–	0.143**	–	0.103**	–	–	–
$Energy_{\alpha}$	–	0.211***	–	0.179***	–	–	–	0.124***	–	0.200***	0.167***	–	0.385***	–	0.151***	–	–	–	–	–	0.167***	0.268***	–	–
RBP_{δ}	–	–	−0.260***	−0.158***	–	–	–	–	–	**−0.310*****	–	–	–	−0.194***	–	−0.180***	–	−0.144***	–	–	–	−0.175***	−0.190***	**−0.410*****
Variance	–	–	–	−0.126***	–	−0.155***	−0.133***	–	–	–	–	–	–	–	–	–	–	–	−0.145***	–	−0.101**	−0.242***	–	−0.157***
$Energy_{\theta}$	–	–	−0.090***	–	–	–	–	–	–	−0.28***	–	–	−0.380***	−0.115***	–	–	–	–	–	−0.239***	–	–	–	−0.133***
$Energy_{\delta}$	–	–	–	–	–	−0.165***	–	–	–	–	–	–	−0.102*	–	**−0.311*****	–	–	–	–	−0.075**	−0.075***	−0.140***	–	–
STD	–	–	–	–	–	0.206***	0.286***	–	0.084***	–	–	–	–	0.121***	–	–	–	–	0.242***	–	–	–	–	–
$ApEn_{\delta}$	–	–	–	–	–	0.120***	–	–	–	–	–	0.065**	–	–	–	–	–	–	0.079*	–	–	–	–	0.145***
$ApEn_{\beta}$	–	–	0.211***	0.145***	–	–	–	0.142***	–	–	0.126***	0.270***	**0.475*****	–	–	–	–	–	–	–	–	–	–	–
$ApEn_{\alpha}$	–	–	−0.132***	–	–	–	–	–	–	0.110***	–	–	–	–	–	**−0.306*****	–	−0.293***	–	–	0.213***	–	–	–
$ApEn_{\beta}$	–	–	0.042***	0.037**	0.023*	–	–	–	–	–	0.136***	–	0.299***	–	–	–	–	–	–	–	–	0.061***	0.080***	–
$Energy_{\beta}$	–	–	0.101***	0.128***	0.095***	–	−0.046*	–	–	–	–	0.091**	–	–	–	–	–	–	0.117***		0.227***	–	–	–
IQR	–	–	0.044***	0.207***	–	–	–	–	–	–	–	–	–	–	0.061**	–	–	–	–	–	0.191***	**0.368*****	–	0.260***
RBP_{β}	–	–	0.257***	0.052*	–	–	–	–	–	–	–	0.136***	0.121***	0.064**	–	–	–	–	–	–	–	–	–	0.153***
RBP_{α}	–	–	–	–	–	–	–	–	–	–	–	–	–	–	–	–	–	–	0.224***	–	–	–	**0.520*****	0.191***
$SamplEn_{\gamma}$	–	–	–	–	–	–	–	–	–	–	–	–	–	–	–	–	**0.399*****	–	–	–	–	–	–	–
$PermEn_{\gamma}$	–	–	–	–	–	–	–	–	–	–	–	–	**−0.363*****	–	–	–	–	–	–	−0.297***	–	–	–	–
Skewness	–	–	–	−0.054**	–	–	–	–	–	–	–	–	–	–	0.074***	–	–	–	–	–	–	–	–	–
$TsalEn_{\theta}$	–	–	–	0.044***	–	–	–	–	–	–	–	0.052**	–	–	–	–	–	–	0.048**	–	–	–	–	–
$TsalEn_{\delta}$	–	–	0.029	–	–	–	0.046**	–	–	–	–	–	–	–	–	–	–	–	–	–	–	–	–	–
$TsalEn_{\beta}$	–	–	–	–	–	–	–	–	–	–	–	–	–	–	–	–	–	–	–	–	0.047**	–	–	–
$TsalEn_{\gamma}$	–	–	–	–	–	–	–	–	–	–	–	–	–	–	–	–	–	–	0.040*	–	–	–	–	–
$TsalEn_{\alpha}$	–	–	–	–	–	–	–	–	–	–	–	–	–	–	–	–	–	–	–	–	–	–	–	–

$^{*}p$-value < 0.05, $^{**}p$-value < 0.01, $^{***}p$-value < 0.001.

Table 6
A comparative representation of the most recent studies that have associated the MMSE score with the EEG feature changes due to AD progression.

Author	Year	Dataset	Dataset duration	Features	Results
Fraga et al. [19]	2013	27 controls 27 mild AD 22 moderate AD	304 s/subject = 6 h, 25 min	amplitude modulation	↓ beta band amplitude modulation as AD progresses ↑ theta band amplitude modulation as AD progresses
Yang et al. [4]	2013	15 MCI 69 mild AD 24 moderate AD	30 s/subject = ∼1 h	multiscale entropy	↓ multiscale entropy (low τ) of occipitoparietal region as AD progresses
Garn et al. [22]	2015	118 probable AD patients	158 s/subject = 5 h, 11 min	relative band power, coherence, canonical correlation, auto-mutual information (AMI), Shannon entropy (ShEn), Tsallis entropy (TsE)	↑ theta power in AD compared to CN coherence and canonical correlation correlated with MMSE ↑relative theta power in AD ↑auto-mutual information in AD
Waser et al. [5]	2016	79 probable AD patients	180 s/subject = 3 h, 57 min	coherence, partial coherence, phase shift, Granger causality, conditional Granger causality, canonical correlation, dynamic canonical correlation, cross-mutual information	$R^2 = 0.3 \sim 0.386$ for coherence, partial coherences, phase shift, Granger causalities, conditional Granger causalities, and the cross-mutual information ↑ of EEG synchrony for MMSE >20 ↓ of EEG synchrony for MMSE <20
Coronel et al. [13]	2017	79 mild to moderate AD patients	168 s/subject = 3 h, 41 min	auto-mutual information (AMI), Shannon entropy (ShEn), Tsallis entropy (TsE), multiscale entropy (MsE) and spectral entropy (SpE)	$R^2 = 0.30 \sim 0.46$ higher at T7 and F7 ↑ of AMI, SpE, MsE as AD progresses
Tzimourta et al.	2018	10 controls 8 mild AD 6 moderate AD	∼16 min/subject = 6 h, 30 min	Mean, Variance, Skewness, Kurtosis, Standard deviation, IQR, Energy, Relative Band Power, Shannon Entropy, Approximate Entropy, Permutation entropy (PermEn), Tsallis entropy, Multiscale entropy, Sample entropy (SamplEn)	$R^2 = 0.202 - 0.542$, higher at O2 and F4 $R^2 = 0.365$ for posterior cluster ↓ PermEn of δ rhythm in AD, ↓ SamplEn of θ rhythm in AD ↑ Relative θ power in AD

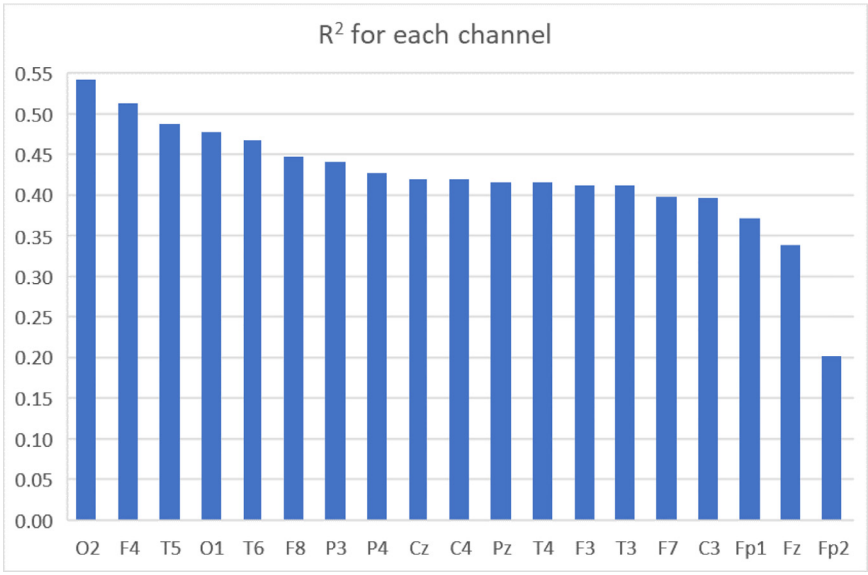

Fig. 3. Distribution of the obtained R^2 after the Multiregression Analysis for each EEG channel. Electrodes O2 and F4 shows the highest correlation with MMSE score and thus the severity of the Alzheimer's Disease, whereas the lowest association with MMSE is shown in the EEG features extracted from electrode Fp2.

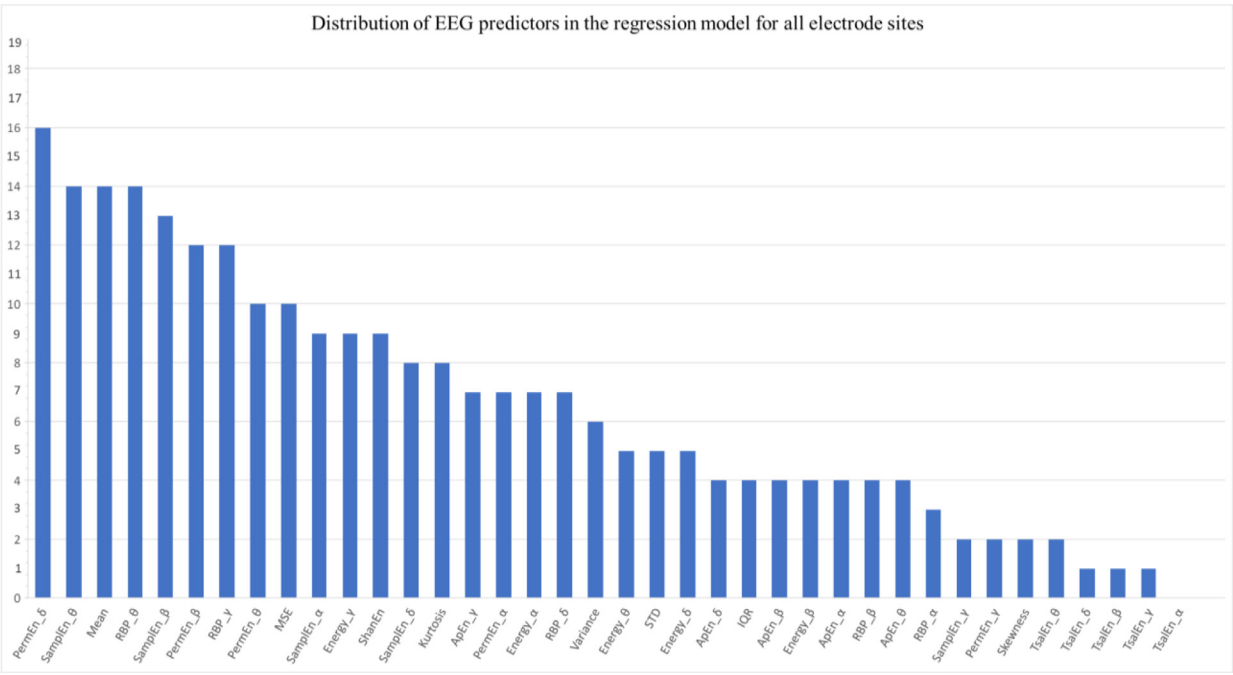

Fig. 4. Representation of the contribution of significant predictors in the final regression model of 19 electrodes. Each bin corresponds to a different EEG feature and each number in y-axis represents an electrode. $PermEn_\theta$ is the feature that contributed the most in the final regression model of 16 electrodes, whereas Tsallis Entropy in all of the 5 five bands contributed the least.

mild AD and 6 patients with moderate AD. Multiregression linear analysis is performed to examine the best model of EEG features that predicts the MMSE score and ANOVA test is also conducted to evaluate the significance of the regression models. The proposed analysis shows significant results in the association of MMSE score with certain complexity EEG features. Statistically significant results of Multiregression linear analysis in terms of Multiple Correlation Coefficient (R^2) indicated high association of the MMSE with simple EEG features and particularly Relative band power, Sample Entropy and Permutation Entropy, whereas Approximate Entropy, Shannon Entropy and Multiscale Entropy are also significant measures in the regression models of many electrode sites.

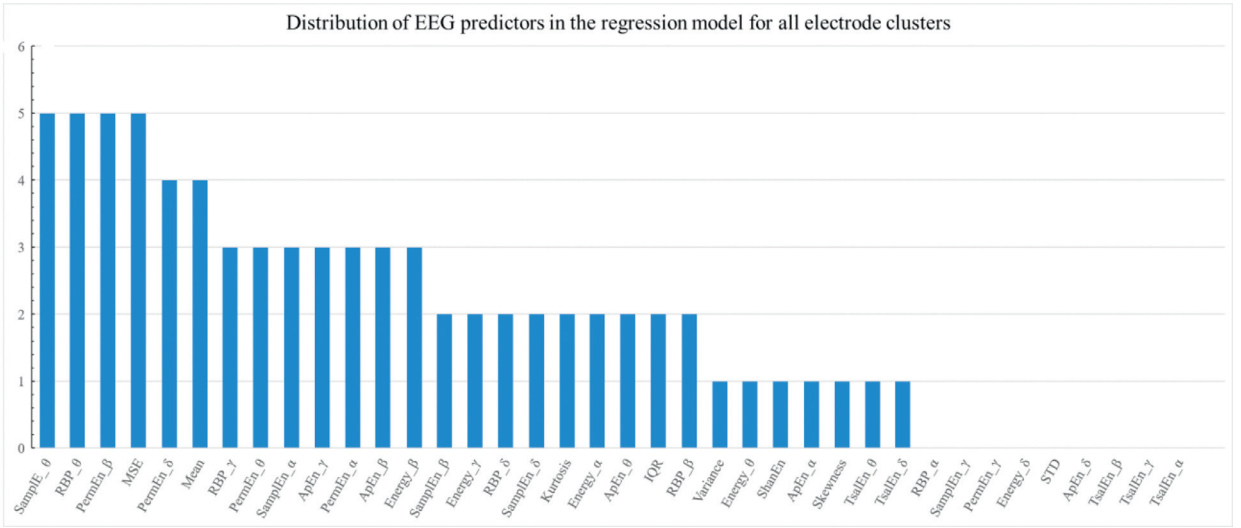

Fig. 5. Representation of the contribution of significant predictors in the final regression model of 5 electrode clusters. Each bin corresponds to a different EEG feature and each number in y-axis represents a cluster. $SamplEn_\theta$, RBP_θ, $PermEn_\beta$ and MSE are the features that contributed the most in the final regression model of all the five electrode clusters. Nine features did not shown in the final regression model of any electrode cluster.

Results of the proposed analysis are consistent with previous studies ([17, 18, 16, 3]) concerning the decline of Relative Power of α, β and γ rhythm in AD patients and the dominance of low frequency bands (δ and θ rhythm). RBP_δ and RBP_θ are negatively correlated with MMSE score variation, whereas RBP_α, RBP_β, *and* RBP_γ showed positive correlation. Posterior and left-sided and right-sided temporal area have also shown higher correlation with AD from other brain regions as have been inferred to previous studies [11,13].

SamplEn indicated positive correlation with MMSE for θ, α, β and γ rhythm. Concerning δ rhythm, SamplEn is positively correlated for O1, O2 and Pz sites, while it is negatively correlated for left-sided temporal cluster and Fp1, F3, F4, F7 and T3 electrode sites. Abasolo et al. 2006 [11] also reported significant decrease of SamplEn at O1, O2, P3 and P4 sites in AD patients. An increased complexity of lower bands of independent neural regions of frontal and temporal/left brain sides, may indicate disintegration of different brain parts and of interneuronal corporation [21].

PermEn is a significant predictor of the MMSE score and has been previously reported ([8, 7]) that PermEn is decreased in AD patients. In this study, PermEn calculated for the entire frequency spectrum, is also decreased as the MMSE score takes low values. However, PermEn calculated for each EEG rhythm separately, shows positive correlation with MMSE for δ and θ rhythm in general and negative correlation with MMSE score for β rhythm and γ rhythm. Concerning PermEn_α, results for each electrode site showed positive correlation in O1, O2, P4, T4 and F8 and negative correlation for Cz and Fz electrode sites. Results for each electrode cluster showed negative correlation only for central regions and positive correlation in temporal/left and posterior cluster. This is a significant outcome, which assumes that the irregularity of β and γ rhythm in AD patients is increased and is consistent with previous study [28], while δ and θ rhythm are more predictable. These differences among different brain structures shows diversity in neural network communication and reveals less efficient brain organization.

$ApEn_\delta$, $ApEn_\theta$ and $ApEn_\beta$ are positively correlated with MMSE score, meaning that $ApEn_\delta$, $ApEn_\theta$ and $ApEn_\beta$ decreases as MMSE score gets lower values. As mentioned before, high values of ApEn are an indicator of more complex and chaotic system, whereas low values indicate a more regular and more predictable signal. This result is consistent with prior literature that there is a decline of α rhythm in resting state EEG and appearance of θ and δ rhythm [22–26]. However, former studies ([8, 9, 12]) reported lower EEG complexity in AD patients, examining ApEn in the entire spectrum and each frequency band is not separately analyzed. Results of this study reveals the correlation of MMSE score with the decrease of complexity in δ and θ rhythm specifically, as expressed by Approximate entropy. Therefore, EEG waveforms of more severe AD present less complex θ or δ rhythm and more predictable dynamics. On the other hand, $ApEn_\gamma$ showed negative correlation with MMSE score in Fp1, C3, C4, T4, T6, Pz, and O2 electrode sites as well as in anterior, posterior and temporal/right cluster. A recent study [29], had also reported enhanced γ activity in AD patients during resting-state EEG recording mainly in the midline frontal, central-parietal and occipital areas.

With regard to ShanEn and TsalEn, the left-sided temporal brain with ShanEn and TsalEn [13], and parietal regions showed most significant results in previous studies [15]. However, in this study TsalEn is not a great predictor of MMSE score (Beta weight ranging from 0.029 to 0.052), as it has been previously reported [13]. TsalEn showed positive correlation in all frequency bands and is chosen based on its Pearson correlation only in the significant regression models of F3, O1, T4, F8 and in the model of left temporal and right temporal cluster. On the other hand, ShanEn of the entire frequency

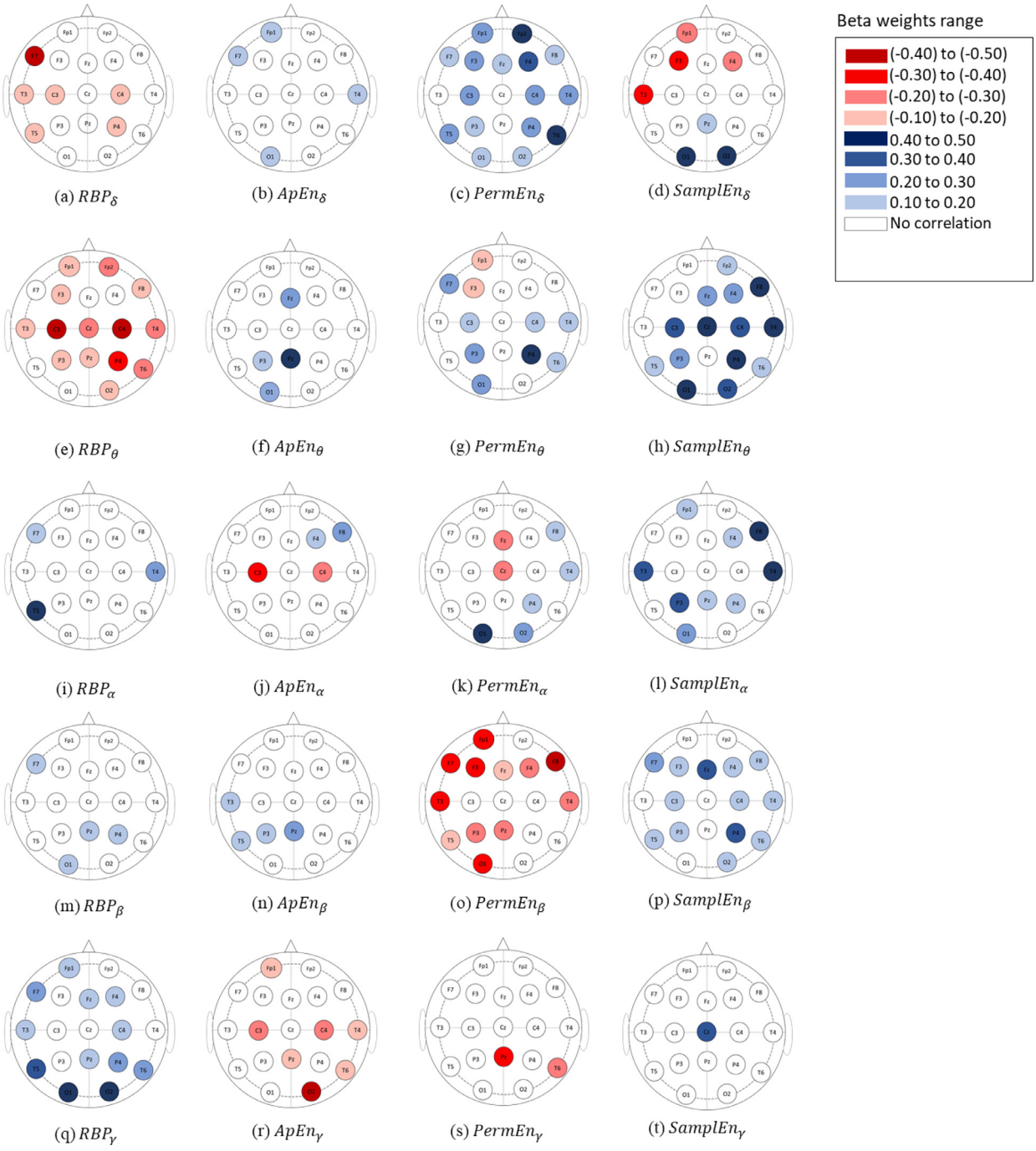

Fig. 6. Correlation of the most significant EEG markers with MMSE according to the obtained Beta weights of the Multiregression Analysis. Blue color represents a positive correlation of the predictor with MMSE score, whereas red color represents negative correlation of the predictor with MMSE score. White color represents no correlation of the predictor of each electrode with MMSE score.

spectrum is a good predictor in this study, showed positive correlation with MMSE. Also, ShanEn is chosen as a significant predictor in 9/19 channels with greatest correlation in Cz and central region.

Yang et al. in [4] reported that MSE correlates with the progression of the Alzheimer's Disease and for low scales of τ, the MSE increases as the MMSE score increases; hence, mild and very mild AD patients show more complex EEG recordings. In this study, τ is assigned to 5 and MSE is also positively correlated with MMSE. This finding suggests that it is easier to predict EEG background activity in AD patients than in control subjects [30]. Moreover, MSE shows good correlation with

MMSE score in 10/19 channels and in four electrode clusters the greatest correlation is shown in temporal/right region and O1 site.

Statistical EEG features have also been good predictors of MMSE variation. Mean, and Kurtosis showed negative correlation with the dependent variable in 14 and 8 electrode sites respectively and 4 and 2 electrode clusters. IQR and Standard deviation indicated positive correlation in less electrode sites (5 and 4 respectively). A comparison of the proposed study with previous studies is shown in Table 6.

5. Conclusion

Alzheimer's Disease is a chronic neurological disorder affecting the cognitive state of a large group of elderly people worldwide. Over the past few years, a great interest on the progress of the disease severity, as expressed from MMSE score, with features extracted from EEG recordings has emerged. To the best of the author's knowledge, this is the first comprehensive study combining simple complexity EEG features of EEG bands and statistical features to create a regression model that predicts MMSE score variation. The combination of several linear and non-linear features can provide complementary information about the association of EEG markers with MMSE score. Previous reported studies have examined the correlation of MMSE with entropy measures calculated mainly in the entire frequency spectrum. In this study, the EEG complexity among EEG bands showed that SamplEn and PermEn indicated the best results as predictors of MMSE score in most of the electrode sites. Also, ApEn, MSE and ShanEn showed good correlation with MMSE score variation. However, a drawback of the proposed study is the small number of patients and the difficulty of finding AD patients without neurological comorbidities (depression, epilepsy, etc.) that may mislead the obtained models. Future directions of the proposed work will focus on the association of other proposed in the literature EEG markers with MMSE score. Furthermore, an extension of the study to Mild Cognitive Impairment (MCI) patients may be useful for the progression of the disease. Thus, in a subsequent analysis EEG recording acquired from more patients would be analyzed and more feature combinations should be examined to improve the method's statistical results.

Acknowledgments

This research has been co-financed -via a programme of State Scholarships Foundation (IKY)- by the European Union (European Social Fund - ESF) and Greek National Funds (grant no. MIS 5000432)through the action entitled "Strengthening Human Resources Research Potential via Doctorate Research – 2nd Cycle" (Contract No. 2018-050-0502-14226) in the framework of the Operational Programme "Human Resources Development Program, Education and Lifelong Learning" of the National Strategic Reference Framework (NSRF) 2014 – 2020.

Conflict of interest

None.

References

[1] Serrano-Pozo A, Frosch MP, Masliah E, Hyman BT. Neuropathological alterations in Alzheimer disease. Cold Spring Harb Perspect Med 2011;1(1).
[2] Martin Prince MP, Wimo A, Guerchet M, Ali G-C, Wu Y-T, World Alzheimer Report 2015 The Global Impact of Dementia An analysis of prevalence, incid ence, cost and trends, London, 2015.
[3] Cassani R, Estarellas M, San-martin R, Fraga FJ, Falk TH. Systematic review on resting-state EEG for Alzheimer's disease diagnosis and progression assessment. Dis Markers 2018;2018:1–47.
[4] Yang AC, Wang S, Lai K, Tsai C, Yang … C, Fuh J. Cognitive and neuropsychiatric correlates of EEG dynamic complexity in patients with Alzheimer's disease. Prog Neuro-Psychopharmacology Biol Psychiatry 2013;47:52–61.
[5] Waser M, Garn H, Schmidt R, Benke T, Dal-Bianco P, …, Deistler M. Quantifying synchrony patterns in the EEG of Alzheimer's patients with linear and non-linear connectivity markers. J Neural Transm 2016;123(3):297–316.
[6] Falk TH, Fraga FJ, Trambaiolli L, Anghinah R. EEG amplitude modulation analysis for semi-automated diagnosis of Alzheimer's disease. EURASIP J Adv Signal Process 2012;2012:1–9.
[7] Deng B, Cai L, Li S, Wang R, Yu H, … JWang. Multivariate multi-scale weighted permutation entropy analysis of EEG complexity for Alzheimer's disease. Cognit Neurodyn 2017;11(3):217–31.
[8] Tylová L, Kukal J, Hubata-Vacek V, Vyšata O. Unbiased estimation of permutation entropy in EEG analysis for Alzheimer's disease classification. Biomed Signal Process Control 2018;39:424–30.
[9] Abásolo D, Hornero R, Espino P. Approximate entropy of eeg background activity in alzheimer's disease patients. Intell Autom Soft Comput 2009;15(4):591–603.
[10] Jeong J, Kim SY, Han SH. Non-linear dynamical analysis of the EEG in Alzheimer's disease with optimal embedding dimension. Electroencephalogr Clin Neurophysiol 1998;106(3):220–8.
[11] Abásolo D, Hornero R, Gómez C, García M, López M. Analysis of EEG background activity in Alzheimer's disease patients with Lempel-Ziv complexity and central tendency measure. Med Eng Phys 2006;28(4):315–22.
[12] Labate D, La Foresta F, Morabito G, Palamara I, Morabito FC. Entropic measures of EEG complexity in alzheimer's disease through a multivariate multiscale approach. IEEE Sens J 2013;13(9):3284–92.
[13] Coronel C, Garn H, Waser M, Deistler M, Benke T, …, Schimdt R. Quantitative EEG markers of entropy and auto mutual information in relation to MMSE scores of probable Alzheimer's disease patients. Entropy 2017;19(3):1–14.
[14] Dauwels J, Vialatte F, Musha T, Cichocki A. A comparative study of synchrony measures for the early diagnosis of Alzheimer's disease based on EEG. Neuroimage 2010;49(1):668–93.
[15] Garn H, Waser M, Deistler M, Benke T, Dal-Bianco P, …, Schimdt R. Quantitative EEG markers relate to Alzheimer's disease severity in the Prospective Dementia Registry Austria (PRODEM). Clin Neurophysiol 2015;126(3):505–13.

[16] Kwak YT. Quantitative EEG findings in different stages of Alzheimer's disease. J Clin Neurophysiol 2006;23(5):457–62.
[17] Coben LA, Danziger W, Storandt M. A longitudinal EEG study of mild senile dementia of Alzheimer type: changes at 1 year and at 2.5 years. Electroenc Clin Neurophysiol 1985;61(2):101–12.
[18] Penttilä M, Partanen JV, Soininen H, Riekkinen PJ. Quantitative analysis of occipital EEG in different stages of Alzheimer's disease. Electroenc Clin Neurophysiol 1985;60(1):1–6.
[19] Fraga FJ, Falk TH, Kanda PAM, Anghinah R. Characterizing Alzheimer's disease severity via resting-awake EEG amplitude modulation analysis. PLoS One 2013;8(8).
[20] Al-Qazzaz NK, Ali SHBM, Ahmad SA, Chellappan K, Islam MS, Escudero J. Role of EEG as biomarker in the early detection and classification of dementia. Sci World J 2014.
[21] Czigler B, Csikos D, Hidasi Z, Gaal Z, Csibri E, Molnar M. Quantitative EEG in early Alzheimer's disease patients - Power spectrum and complexity features. IntJ Psychophysiol 2008;68(1).
[22] Garn H, Waser M, Deistler M, Schmidt R, Dal-Bianco P, ..., Benke T. Quantitative EEG in Alzheimer's disease: cognitive state, resting state and association with disease severity. Int J Psychophysiol 2014;93(3):390–7.
[23] Pincus SM. Approximate entropy as a measure of system complexity. Proc Natl Acad Sci USA 1991;88:2297–301.
[24] Bandt C, Pompe B. Permutation entropy: a natural complexity measure for time series. Phys Rev Lett 2002;88(17):4.
[25] Tsallis C. Possible generalization of Boltzmann–Gibbs statistics. J Stat Phys 1988;52(Nos. 1/2):479–87.
[26] Costa M, Goldberger AL, Peng CK. Multiscale entropy analysis of biological signals. Phys Rev E - Stat Nonlinear Soft Matter Phys 2005;71(2):1–18.
[27] Richman JS, Moorman JR. Physiological time-series analysis using approximate entropy and sample entropy. Am J Physiol Circ Physiol 2000;278(6):H2039–49.
[28] Frantzidis CA, Vivas AB, Tsolaki A, Klados MA, Tsolaki M, Bamidis PD. Functional disorganization of small-world brain networks in mild Alzheimer's disease and amnestic Mild cognitive impairment: an EEG study using Relative Wavelet Entropy (RWE). Front Aging Neurosci 2014;6(August):1–11.
[29] Wang J, Fang Y, Wang X, Yang H, Yu X, Wang H. Enhanced gamma activity and cross-frequency interaction of resting-state electroencephalographic oscillations in patients with Alzheimer's disease. Front Aging Neurosci 2017;9(JUL):1–7.
[30] Escudero J, Abásolo D, Hornero R, Espino P, López M. Analysis of electroencephalograms in Alzheimer's disease patients with multiscale entropy. Physiol Meas 2007;28(12).

Katerina D. Tzimourta was born in Thessaloniki, Greece (1991). She received the diploma degree in Informatics and Telecommunications Engineering from the University of Western Macedonia, Kozani, Greece in 2015. She is currently a Ph.D. Student in the Medical Physics Laboratory, University of Ioannina, Greece. Her research interests are oriented towards biosignal processing, machine learning and wearable devices.

Theodora Afrantou is a neurologist since 2004 with a doctoral degree in epilepsy. She received postgraduate training at the Video-EEG unit at National Hospital, Queen's Square in London. She is currently working as a Consultant of Neurology and is the Head of the Electroencephalography Lab and the Video-EEG Unit at B' Dept of Neurology, AHEPA University Hospital in Thessaloniki, Greece.

Panagiotis Ioannidis graduated from Medical School (1992) from Aristotle University of Thessaloniki (A.U.TH.), obtained his residency in Neurology (2001),his specialization in dementia from University College London (2002). He received his PhD from A.U.TH. (2006). He is Associate Professor of Neurology at the Medical School of A.U.TH., AHEPA Hospital and responsible for the Outpatient Dementia and relevant disorders clinic.

Maria Karatzikou was born in Thessaloniki in 1986 and graduated from Department of Medicine, University of Thessaly in 2010. She is currently in her last year of residency in Neurology at the B' Neurological Department of the University Hospital AHEPA in Thessaloniki, Greece, completing her training in neurophysiology laboratory (EEG, EMG).

Alexandros T. Tzallas is currently Assistant Professor of Biomedical Engineering, Department of Informatics and Telecommunication, University of Ioannina. He is also affiliated academic partner of the Center for Research & Technology Hellas/Information Technologies Institute (CERTH/ITI). His research interests include EEG, wearable devices, biomedical signal and image processing, biomedical engineering, decision support and medical expert systems and biomedical applications.

Nikolaos Giannakeas graduated from the Physics Department, University of Ioannina, in Greece. In 2011 he defended his Ph.D. in bioinformatics. He has more than 10 years of experience in European and National projects in the fields of signal/image processing, machine learning, and decision support, focusing on bioinformatics and biomedical engineering. Currently, he is Assistant Professor in University of Ioannina.

Loukas Astrakas is Assistant Professor in Medical Physics, University of Ioannina, Greece. He has been educated in Physics (B.Sc., University of Athens), Medical Physics (M.Sc., University of Patras) and spectroscopy (Ph.D., NCSR "Demokritos"). He was trained at Harvard University (postgraduate fellow) and Ioannina University (Marie Curie fellow). His research interests include biomedical applications of magnetic resonance and structural/functional brain imaging.

Pantelis Angelidis received his diploma and his Ph.D. from the School of Electrical Engineering, Aristotle University of Thessaloniki, Greece (1989 and 1993 respectively). He is Professor on Biomedical Signal Processing at the Department of Informatics and Telecommunications Engineering, University of Western Macedonia, Kozani, Greece. He focuses on digital technologies for preventive health and active ageing.

Evripidis Glavas graduated from University of Ioannina, Greece (1983) with a Diploma in Physics. He received his Ph.D. degree from University of Sussex in 1988. He had extensive experience in basic and applied research, in producing innovative products and in industrial standards certification. He is currently Professor at the Informatics & Telecommunications Department of the University of Ioannina.

Nikolaos Grigoriadis is Professor of Neurology at the Aristotle University of Thessaloniki and Head of the B' Dept of Neurology, AHEPA University Hospital, the MS Centre and the Laboratory of Experimental Neurology and Neuroimmunology. He has been specialized in clinical and experimental Neuroimmunology and CNS immunopathology in a number of research centers and institutions abroad.

Dimitrios G. Tsalikakis received the Diploma degree in Mathematics from University of Ioannina and his PhD in cardiac modeling (2006). He is a Lecturer in the Dept. of Engineering Informatics and Telecommunications, University of Western Macedonia, Greece. His research interests include cardiac modeling, monophasic action potential analysis, automated systems analysis, virtual instrumentation, scientific computing, mathematical models and differential equations.

Markos G. Tsipouras received the diploma degree in Computer Science, M.Sc. and Ph.D. in biomedical informatics from University of Ioannina, Greece (1999, 2002 and 2008, respectively). He is an Associate Professor in the Dept. of Informatics and Telecommunications Engineering, Greece. His research interests include digital biosignals processing and images, medical informatics, data mining, fuzzy logic and machine learning.